

## Feasibility Assessment of Bolometry as Impurity Transport Study Tool for the Stellarator W7-X

D. Zhang<sup>1</sup>, R. Dux<sup>2</sup>, R. Burhenn<sup>1</sup>, H. Thomsen<sup>1</sup>, H. Jenzsch<sup>1</sup>, R. König<sup>1</sup>, T. Sunn Pedersen<sup>1</sup> <sup>1</sup>*Max-*

<sup>1</sup>*Planck-Institut für Plasmaphysik, 17491 Greifswald, Germany*

<sup>2</sup>*Max-Planck-Institut für Plasmaphysik, 85748 Garching, Germany*

### Introduction

The stellarator W7-X, just being in the commissioning state, will begin its first operation phase in about one year [1]. Intrinsic impurities possibly released from the plasma facing components (PFC) are expected to be predominantly C, Fe, O and possibly Cu. They are generated by sputtering due to highly energetic particles, might penetrate into the core plasma region and lead to high radiative losses. The associated impurity transport processes in stellarators are only partially understood. Whether the impurity transport in the core region is predominant by neoclassical transport, as for the case of the background gas in W7-AS ( $Te \geq 0.5$ keV) [2], or by turbulence induced ‘anomalous’ transport is still an open issue. Active impurity injection methods [3-4], like gas-puff, laser blow-off or pellet injection, are indispensable for relevant studies. At W7-X, several diagnostics are dedicated to this purpose [5,6]. The bolometers [7], in total eleven systems in the long-term plan, aim basically to measure the total plasma radiation, mainly originating from impurities, at different poloidal and toroidal positions for investigating 3D radiation features. Soon, a horizontal bolometer camera (HBC) and a vertical one (VBC) will be installed for monitoring the plasma at the triangular cross section. They are equipped with arrays of both blank and optically filtered gold-foil detectors (in HBC: 32 channels each; in VBC: 40 blank- and 8 filtered ones) in order to obtain more information about the spectral distribution of the whole impurity radiation content, especially from high-Z species. The filtered channels are covered with  $10\mu\text{m}$ -Be-foils and only sensitive to soft X-rays ( $>750\text{eV}$ ), which are emitted by high-Z elements in the core region. These channels are overall called hereafter as SXR-bolometer. This present paper focuses on the investigation of the suitability of these channels for impurity transport studies.

### Simulation of SXR-bolometer signals

The SXR-channels in the HBC have almost identical lines of sight (LoS) to those of the blank detectors as shown in reference [7], providing directly the radiation level in the core region and at the scrape-off layer (SOL). The simulations are performed for these channels. An artificial experiment with active Fe-injection is considered: A steady-state background plasma of hydrogen with peaked density and temperature profiles,  $n_e(0)=1.0 \cdot 10^{20}\text{m}^{-3}$  and  $T_e(0)=9.4\text{keV}$  on axis, is assumed. The ‘standard’ magnetic configuration with a minor radius of  $a=51.8\text{cm}$  is being used as a basis of the investigation. The Fe-impurity injection is assumed to take place at the plasma

wall ( $r_w=72\text{cm}$ ) with a uniform source distribution on the whole wall surface and has a constant flux rate of  $1.0 \cdot 10^{22}$  atoms/s for a pulse duration of 1s. The injected Fe-neutrals become ionized and undergo parallel transport, radial diffusion and convective motion in the SOL and also penetrate into the core region. The core plasma inside the last closed flux surface (LCFS) as well as the SOL are divided into in total 28 radial zones (onion shell model) for the numerical simulations; the former is based on the flux surface contours while the latter is defined by linear extrapolation of the LCFS.

Signal of each channel is a line-integral along its own LoS, i.e.  $s(l) = \sum_{nr} \varepsilon(nr)g(nr,l)$ , with  $g(nr,l)$

representing the geometric weight of channel  $l$  in the plasma zone  $nr$ ,  $r$  the effective radius and  $\varepsilon(nr)$  the local SXR-emissivity. A 1D-model is used to describe the impurity propagation process; the relevant parameters, the emissivity  $\varepsilon$ , the ion density  $n_Z$  and both transport coefficients, the diffusion coefficient  $D$  and convection velocity  $V$ , are only functions of  $r$ . The 1D impurity transport equation to

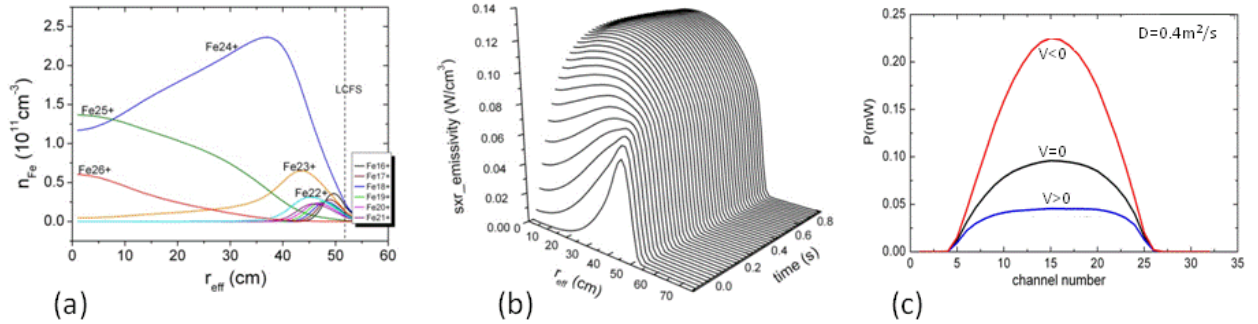


**Fig.1** (a) Radial distribution of the Fe-ions ( $Z=16-26$ ) inside the LCFS at stationary state; (b) the temporal evolution of SXR-emissivity profile after Fe-injection; (c) the maximum channel signals reached at stationary state for  $D=0.4\text{m}^2/\text{s}$  and with different convections ( $V<0$ : red,  $V=0$ : black and  $V>0$ : blue).

be solved reads  $\frac{\partial n_Z}{\partial t} = \frac{1}{r} \frac{\partial}{\partial r} r(D \frac{\partial n_Z}{\partial r} - v n_Z) + Q_Z$ , where  $Q_Z$  includes the sources and sinks of the ions

with charge  $Z$ , which are determined by the ionization and recombination processes of its two neighboring ionization stages,  $n_e S_{Z-1} n_{Z-1} + n_e \alpha_{Z+1} n_{I,Z+1}$ , and itself  $-(n_e S_Z + n_e \alpha_Z) n_Z$ . The set of equations, for  $Z=1-26$ , is solved by STRAHL-code [8] using the ionization- and recombination rate coefficients,  $S_Z$  and  $\alpha_Z$ , from the ADAS database [9]. Reference [8] describes how STRAHL treats the transport in the SOL and which numerical algorithms are used. First neutral particle distribution,

described as  $n_0(r) = n_0(r_w) \frac{r_w}{r} \exp\left(-\int_r^{r_w} \frac{n_e S_0}{v_0} dr\right)$ , with  $v_0$  denoting the thermal velocity of the neutrals

(taken as 1eV), is calculated. The temporal evolutions of the Fe-ion distributions,  $n_z(r,t)$ , are thereby

obtained. Based on these results the local emissivities,  $\varepsilon(r,t) = \sum_Z n_e(r) n_z(r,t) f(Z, T_e)$ , and the channel signals are derived. The radiation loss coefficients,  $f(Z, T_e)$ , are again taken from the ADAS database. Fig.1(a) shows the radial distribution of population densities of the Fe-ions ( $Z=16-26$ ), which are the primary sources of the SXR emission, inside the LCFS after reaching a stationary state; the temporal evolution of the radial SXR-emissivity profiles is shown in Fig.1(b). The transport coefficients used for the figures are  $D=0.4 \text{ m}^2/\text{s}$  and  $V=0 \text{ m/s}$ . Calculations for various  $D$ - and  $V$ -values indicate that the higher the  $D$  value, the higher the signal amplitudes will be for the given source position, i.e. the vessel wall; keeping  $D$  constant and assuming an outward ( $V>0$ ) or inward convection ( $V<0$ ), the signal amplitude can be adjusted to lower or higher levels, respectively (shown in Fig.1(c)). However, the transient signals show a higher sensitivity to the local transport coefficients. They follow approximately functions of  $\sim 1 - \exp(-\Delta t/\tau)$  and  $\sim \exp(-\Delta t/\tau)$  shortly after switching-on and -off of the impurity source. The decay time  $\tau$ , extracted from the signals, spans from 10ms to 100ms with the longest one for the innermost channel. This expected decay times and the signal amplitudes of  $\sim 0.1 \text{ mW}$  are sufficiently large in comparison with the detection limit of  $\sim 0.2 \mu\text{W}$  and the time resolution of 3-5ms of the bolometer system, indicating the possibility to resolve core impurity transport processes on a time scale of interest.

**Estimation of impurity transport coefficients using noisy signals** Based on the simulated channel signals mentioned above, artificial experimental signals are created by adding Gaussian noise with a relative error of 2% to all channels. The original STRAHL-code has been modified to allow iterative calculations with altered  $D$ - and  $V$ -inputs. The radius dependent functions  $D(r)$  and  $V(r)$  are described by Chebyshev polynomials, i.e.  $D(\rho) = \sum C_n T_n(\rho^2)$  and  $V(\rho) = \rho \sum \alpha_n T_n(\rho)$ , respectively, where  $T_n$  is the Chebyshev polynomial of  $n$ th degree,  $T_n(\rho) = \cos(n \cdot \arccos(\rho))$ , and  $\rho = r/a$  the normalized minor radius. These functions implicitly insure the intrinsic features of  $dD/dr = 0$  and  $V(0) = 0$  on plasma axis. The unknown parameters to be determined are the coefficients  $C_n$  and  $\alpha_n$  with  $n \leq 4$  for most moderate profiles. The searched  $D(r)$  and  $V(r)$  are obtained based on least square optimization, i.e. by minimizing  $\chi^2 = \frac{1}{n_l n_t} \sum_l \sum_t \frac{(s_c(l,t) - s_m(l,t))^2}{\sigma^2}$ , with  $s_c$  and  $s_m$  denoting the calculated and the measured (normalized) signals, respectively, and  $\sigma$  the relative errors. The absolute values are not taken into account since they are affected both by the impurity injection rate accuracy as well as the transport parameters in the SOL, about which accurate information usually lacks.

Calculations show that the smallest value of  $\chi^2$  is 0.35. The searched transport coefficients are accordingly obtained as  $D=0.43\text{m}^2/\text{s}$  and  $V=-0.32\cdot(r/a)\text{m/s}$ . The deviation of  $D$  from the expected value ( $0.4\text{m}^2/\text{s}$ ) is due to the numerical resolution associated with the finite iteration steps; the small  $V$ -value

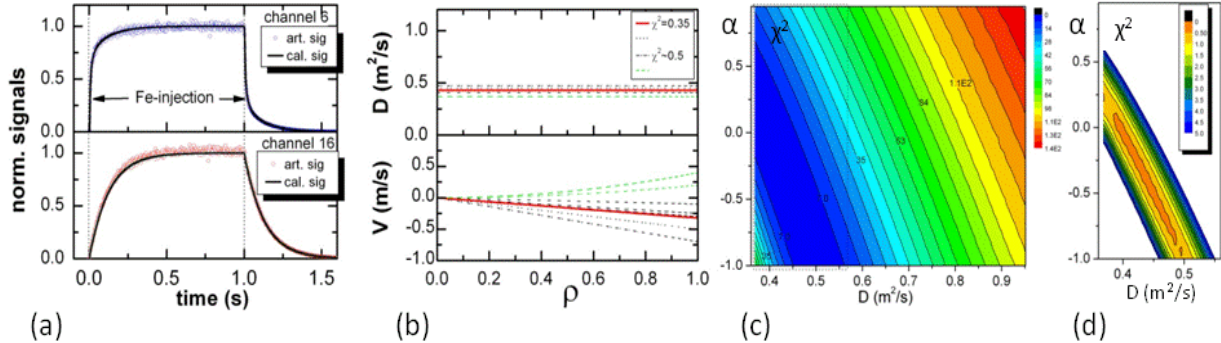


**Fig.2** (a) Fits of the calculated signals to the artificial noisy signals for channel 6 and 16; (b) a comparison of derived transport coefficients profiles  $D(r)$  and  $V(r)$  (in red) with those corresponding to higher  $\chi^2$  ( $\sim 0.5$ ) (in dashed lines); (c) the responses of  $\chi^2$  to the scanned  $D$ - and  $V$ -values in selected ranges; (d) the enlarged range for  $\chi^2 < 5$ .

is coupled with the uncertainty of  $D$ . In Fig.2 the fits to the noisy signals for  $\chi^2=0.35$ , taking channel 6 and 16 as example, are shown in (a), the resulting  $D$ - and  $V$ -profiles are shown in red in (b); also shown are the profiles corresponding to higher  $\chi^2$  ( $\sim 0.5$ ) in order to get an idea of the sensitivity of the results with respect to  $\chi^2$ . The responses of  $\chi^2$  on input values of  $D$ - and  $V$ , with  $V=\alpha\cdot(r/a)$ , are shown in (c) and an enlarged region for the lower  $\chi^2$ -range ( $<5$ ) in (d). All these results demonstrate that the unknown impurity transport coefficients can be deduced from the SXR-bolometer signals measured in the high-Z impurity injection experiments. The accuracy of the results depends on the signal-to-noise level and on the numerical resolution. A good knowledge about the influx rate (e.g. time constant) of impurity injection is also very important, which should be fed into the algorithm for performing more accurate signal predictions.

## References

1. T.S. Pedersen, this conference (41th EPS Berlin), O.xxx
2. M Hirsch *et al* 2008 *Plasma Phys. Control. Fusion* **50** 053001
3. R. Burhenn, A. Weller, *Rev. Sci. Instrum.*, **70** (1999) 603
4. Shigeru Sudo *et al*., *Plasma Phys. Control. Fusion* **55** (2013) 095014
5. R. König, *et al.*, *Rev. Sci. Instrum.* 83, (2012) 10D730
6. H. Thomsen *et al.*, This conference (41th EPS Berlin), P1.075
7. D. Zhang, *et al.*, *Rev. Sci. Instrum.* **81** (2010) 10E134
8. R. Dux, IPP report 10/30 (2006); K. Behringer, JET-R(87)08
9. H.P. Summers, ADAS, Rep. JET-IR 06 (1994)